Available online at www.sciencedirect.com
ScienceDirect
Carbohydrate Polymers 73 (2008) 8–17
Carbohydrate Polymers
www.elsevier.com/locate/carbpol

Comparative study on the films of poly(vinyl alcohol)/pea starch nanocrystals and poly(vinyl alcohol)/native pea starch

Yun Chen [a,b], Xiaodong Cao [a], Peter R. Chang [a,*], Michel A. Huneault [c]

[a] *Bioproducts and Bioprocesses National Science Program, Agriculture and Agri-Food Canada, 107 Science Place, Saskatoon, SK, Canada S7N 0X2*
[b] *Research Centre for Medical and Structural Biology, School of Basic Medical Science, Wuhan University, Wuhan 430071, China*
[c] *Industrial Materials Institute, National Research Council Canada, 75, de Mortagne, Boucherville, Que., Canada J4B 6Y4*

Received 10 September 2007; received in revised form 16 October 2007; accepted 25 October 2007
Available online 4 November 2007

Abstract

Pea starch nanocrystals (PSN) dispersion containing nanocrystals in a range of 30–80 nm was prepared from native pea starch (NPS) granules by acid hydrolysis. Two series of films were prepared by blending poly(vinyl alcohol) (PVA) with NPS and PSN, respectively. The effects of NPS and PSN on the structure and properties of the resulting films were comparatively investigated by FTIR, XRD, SEM, and testing of light transmittance, tensile, and moisture uptake. The light transmittance (Tr), tensile strength (σ_b), and elongation at break (ε_b) of the PVA/NPS films were lower than that of PVA film and decreased with an increase in NPS content. However, the PVA/PSN nanocomposite films containing 5 and 10 wt% of PSN content exhibited improved physical properties over the PVA film. The PVA/PSN films showed higher Tr, σ_b, and ε_b, and lower moisture uptake (Mu) than the corresponding PVA/NPS films with the same component ration. For example, the values of Tr, σ_b, ε_b, and Mu of the PVA/PSN film containing 10 wt% of PSN content were 91%, 40 MPa, 734% and 71%, respectively; while those of the corresponding PVA/NPS film were 69%, 35 MPa, 579% and 73%, respectively. The results revealed that PSN, comparing with NPS, had much smaller sizes and dispersed more homogeneously in PVA matrix, resulting in stronger interactions with PVA. New applications of native pea starch and its nanocrystals as low-cost fillers were explored in this work, and PSN exhibited greater potential than NPS to improve the properties of PVA-based composites.

Keywords: Pea starch; Poly(vinyl alcohol); Nanocrystals; Blend; Nanocomposite; Film

1. Introduction

Poly(vinyl alcohol) (PVA) is the largest synthetic water-soluble polymer produced in the world (Ramaraj, 2007a). It is also a versatile polymer with many industrial applications because of its biodegradability, biocompatibility, chemical resistance, and excellent physical properties (Paradossi, Cavalieri, Chiessi, Spagnoli, & Cowman, 2003; Zhai, Yoshii, & Kume, 2003). It has been reported that PVA with an average molecular weight as high as 10^6 could be completely degraded by soil bacteria, especially by *Pseudomonads* (Lenz, 1993). However, the degradation process of pure PVA is quite slow, particularly under anaerobic conditions (Pšeja, Charvátová, Hruzík, Hrnčiřík, & Kupec, 2006); and the degradation rate strongly depends on the residual acetate groups (Corti, Cinelli, D'Antone, Kenawy & Solaro, 2002). Another shortcoming of PVA is its high-cost, which has to compete with low-cost thermoplastic materials like polyethylene, polypropylene, and poly(vinyl chloride) in practical applications (Ramaraj, 2007b). Hence, a potential solution to enhance the biodegradation rate and lower the cost of PVA lies in preparing composites with more biodegradable, cheaper, and easily processable fillers or polymers. For example, many kinds of PVA-based biodegradable composites have been prepared by blending PVA with natural polymers such as starch (Follain, Joly, Dole, & Bliard, 2005b; Lawton, 1996; Siddaramaiah, Raj, & Somashekar, 2004), cellulose (Ramaraj, 2006), cellulose

* Corresponding author. Tel.: +1 306 9567637; fax: +1 306 956 7247.
E-mail address: Changp@agr.gc.ca (P.R. Chang).

0144-8617/$ - see front matter
doi:10.1016/j.carbpol.2007.10.015

(Ramaraj, 2006), chitin and chitosan (Jia et al. 2007), soy protein (Su, Huang, Liu, Fu, & Liu, 2007), wheat protein (Zhang, Burgar, Lourbakos, & Beh, 2004), egg protein (Yi, Lu, Guo, & Yu, 2004), lignin (Fernandes, Hechenleitner, Job, Radovanocic, & Pineda, 2006), and sodium alginate (Çaykara & Demirci, 2006), etc. Among the above-mentioned natural polymers, starch is one of the most promising materials for the modification of PVA because of its abundant supply, low-cost, good processability, biodegradability, and ease of physical and chemical modifications (Follain et al., 2005b; Mohanty, Misra, & Hinrichsen, 2000). The following sources of starch have been used to blend with PVA for the preparation of PVA/starch composites: potato (Cinelli, Chiellini, Lawton, & Imam, 2006; Ramaraj, 2007b), corn (Imam, Cinelli, Gordon, & Chiellini, 2005; Zhai et al., 2003), wheat (Follain, Joly, Dole, & Bliard, 2005a; Jayasekara, Harding, Bowater, Christie, & Lonergan, 2004), and sago (Khan, Bhattacharia, Kader, & Bahari, 2006). Noticeably, no work on PVA-based composites using pea starch was reported. However, in the PVA/starch composites, starch is just partially compatible with PVA. It was reported that the tensile strength, elongation at break, and transparency of the PVA/starch composites decreased with an increased starch content (Ramaraj, 2006; Siddaramaiah et al., 2004). In general, the addition of starch into PVA does not improve the physical properties because of the poor compatibility between PVA and starch (Siddaramaiah et al., 2004). Thus, the physical properties of PVA/starch composites need further improvement to meet the demands of extensive applications. Some of the effective means commonly used to modify the PVA/starch composites for the improvement of properties include: (1) using chemically modified PVA or starch instead of native PVA and starch (Nabar, Draybuck, & Narayan, 2006); (2) using chemical or physical modifications to the PVA/starch composites during or after the blending process, such as cross-linking reactions, grafting (Beliakova, Aly, & Abdel-Mohdy, 2004; Khan et al., 2006), and surface modification (Jayasekara et al., 2004). The cross-linking reagents and methods reported in PVA/starch composite were glutaraldehyde (Ramaraj, 2007a), boric acid (Yin, Li, Liu, & Li, 2005), epichlorohydrin (Sreedhar, Chattopadhyay, Karunakar, & Sastry, 2006), radiation (Zhai et al., 2003), and photocross-linking (Follain et al., 2005a). Grafting and cross-linking reactions improve the compatibility between PVA and starch molecules, resulting in the improvement of the mechanical properties, transparency and water-resistivity or swelling properties, while retaining the biodegradability (Nabar et al., 2006; Ramaraj, 2007a; Yin et al., 2005).

In recent years, nanowhiskers and nanocrystals have been prepared from natural polymers and applied to reinforce biodegradable or non-biodegradable polymeric matrix (Lu, Weng, & Zhang, 2004; Paillet & Dufresne, 2001; Samir, Alloin, Gorecki, Sanchez, & Dufresne, 2004). Interestingly, Dufresne and his coworkers reported on the preparation of starch nanocrystals from native waxy maize starch (Angellier, Choisnard, Molina-Boisseau, Ozil, & Dufresne, 2004; Dufresne, Cavaillé, & Helbert, 1996) and potato starch (Dufresne & Cavaillé, 1998) granules, and their utilizations to reinforce natural rubber (Angellier, Molina-Boisseau, & Dufresne, 2005), poly(β-hydroxyoctanoate) (Dubief, Samain, & Dufresne, 1999), and starch (Angellier, Molina-Boisseau, Dole, & Dufresne, 2006). The physical properties of the resulting nanocomposites were improved by the incorporation of starch nanocrystals. Canada is the largest producer (~25% of total world production) and the largest exporter (~40% of the total world exports) of field pea in the world (Ratnayake, Hoover, & Warkentin, 2002). Pea starch and pea protein are the two main products from wet process in the pea industry. The market value for pea starch is relatively low and is affected by the market demand and supply from other sources (Cao, Chen, Chang, & Huneault, 2007). This suggests more attention should be paid to explore new and novel applications of pea starch. Thus, we attempted to introduce pea starch to PVA using two different methods. One method utilized the direct blending of native pea starch with PVA to prepare low-cost biodegradable composites. The other method was involved the preparation of starch nanocrystals from native pea starch by an acid hydrolysis process, followed by the blending of the obtained pea starch nanocrystals with PVA to provide property-enhanced composites. The different effects of native pea starch and pea starch nanocrystals on the structure and properties of the two series of PVA-based composites were comparatively investigated.

2. Experimental

2.1. Materials

Native pea starch (NPS), prepared from Golden Canadian field peas and composed of 35% amylose and 65% amylopectin, was supplied by Nutri-Pea Limited Canada (Portage la Prairie, Canada). Poly(vinyl alcohol) (PVA) with M_w of 1.15×10^5 and minimum degree of hydrolysis of 87% was purchased from BDH Limited (Poole, England). NPS and PVA were vacuum-dried at 50 °C for 24 h before use. Glycerol (99.5% purity) and other chemicals were purchased from Sigma–Aldrich Canada Ltd. (Oakville, Canada) and used without further treatment.

2.2. Preparation of pea starch nanocrystals dispersion

Pea starch nanocrystals (PSN) dispersion was prepared by a previously described method (Angellier et al., 2004) with minor modifications. Briefly, native pea starch (NPS) granules were mixed with 3.16 M H_2SO_4 solution at a starch concentration of 15 wt% in a 500 mL Erlenmeyer flask. The suspensions were then continuously stirred at 100 rpm under 40 °C. After 5 days of hydrolysis, the suspensions were washed by successive centrifugations in distilled water until neutrality was achieved. They were dialyzed for 3 days and then diluted with distilled water

to get a PSN dispersion with a concentration of starch nanocrystals around 2 wt%.

2.3. Preparation of the PVA/NPS and PVA/PSN films

Fabrication of PVA/NPS and PVA/PSN films was based on a convenient solution casting and evaporation process (Ramaraj, 2007b). The solution containing 8.0 wt% of PVA and 2.0 wt% of glycerol was prepared by dissolving PVA and glycerol in distilled water. NPS granules and glycerol were mixed and dispersed in distilled water to obtain a suspension containing 8.0 wt% NPS and 2.0 wt% glycerol. The suspension of NPS was then charged into a round bottom flask equipped with a stirrer and heated at 100 °C for 30 min until the mixture gelatinized. Subsequently, the desired weight of PVA solution was added and stirred for another 30 min at 100 °C. The mixture was then filtered quickly using cellulose sieve, cast in a polystyrene Petri dish and dried at 40 °C overnight. By changing the weight ratio of PVA/NPS such as 95/5, 90/10, 85/15, 80/20, 75/25, 70/30, and 60/40, a series of PVA/NPS films with a thickness of about 0.2 mm was prepared. The films were coded as PVA/NPS-*n*, where *n* is the NPS percent based on PVA. For example, PVA/NPS-10 means the weight ratio of PVA and NPS was 90/10 in the blend films, i.e. the NPS percent based on PVA was 10 wt%. Another series of PVA/PSN films was prepared using PSN dispersion instead of NPS suspension. A designated amount of PVA solution was mixed with PSN dispersion and glycerol at room temperature for 30 min. The mixture was filtered and cast in a polystyrene Petri dish and then dried at 40 °C overnight. The resulting films were coded as PVA/PSN-*n*, where *n* is the percent of PSN-based on PVA. As a control, a PVA film without addition of NPS or PSN was obtained using the same fabrication process of PVA/PSN-*n* series films. The films were kept at room temperature in a conditioning desiccator of 43% relative humidity (conditioned by K_2CO_3 saturated solution) for 7 days before being tested.

2.4. Characterizations

2.4.1. Morphology of the NPS and PSN

The morphology of NPS and PSN was observed by a scanning electron microscope (SEM, S-570, Hitachi, Ibaraki, Japan) and a transmission electron microscope (TEM, CM-10, Philips, Eindhoven, The Netherlands), respectively. The NPS granules were dried in vacuum, coated with gold and then observed with an accelerating voltage of 20 kV by SEM. The TEM specimen of PSN was prepared according to a previously reported method with minor modifications (Putaux, Molina-Boisseau, Momaur, & Dufresne, 2003). After a brief ultrasonic treatment, a drop of a dilute PSN dispersion was deposited onto a glow discharged carbon-coated microscopy grid. A drop of 2% (w/v) uranyl acetate was added and sealed in a container for 2 min. Then the grid was moved from uranyl acetate and dipped into a drop of water. After 1 min, the excess liquid was blotted with filter paper and the remaining film was allowed to dry. The stained specimens were observed by TEM with an accelerating voltage of 100 kV.

2.4.2. FTIR analysis

Attenuated total reflection Fourier transform infrared (ATR-FTIR) spectra of the samples were recorded on a Nicolet 5700 FTIR spectrometer (Thermo Electron Corporation, Waltham, MA, USA). The samples were taken at random from the flat films and data were collected over 16 scans with a resolution of 4 cm^{-1} at room temperature. The NPS and PSN were vacuum-dried at 40 °C and then mixed with KBr, respectively, to laminate for the FTIR analysis in a range of wavenumber from 4000 to 600 cm^{-1}.

2.4.3. XRD analysis

Wide-angle X-ray diffraction patterns of the samples were recorded on a Bruker AXS X-ray diffraction instrument (Bruker AXS Inc., Madison, WI, USA), using Cu K_α radiation ($\lambda = 0.154$ nm) at 40 kV and 30 mA with a scan rate of 4° min^{-1}. The diffraction angle ranged from 4° to 40°.

2.4.4. Morphology of the films

A scanning electron microscope (SEM, S-570, Hitachi, Ibaraki, Japan) was used to observe the morphology of the PVA and blend films. The films were frozen in liquid nitrogen and snapped immediately, and then the cross-sections of the films were coated with gold and observed with an accelerating voltage of 20 kV.

2.4.5. Light transmittance testing

The light transmittance (Tr) of the films with a thickness of 0.2 mm was measured using an ultraviolet–visible (UV–Vis) spectroscope (UV-160A, Shimadzu, Japan) at the wavelength from 200 to 800 nm (Kampeerapappun, Ahtong, Pentrakoon, & Srikulkit, 2007).

2.4.6. Tensile testing

The tensile strength (σ_b) and elongation at break (ε_b) of the films were measured on a universal testing machine (CMT 6503, Shenzhen SANS Test Machine Co. Ltd., Shenzhen, China) at room temperature with gauge length of 5 cm and cross-head speed of 50 mm min^{-1}. An average value of four replicates for each sample was taken.

2.4.7. Moisture uptake testing

The samples used were thin rectangular strips with dimension of 50 mm × 10 mm × 0.2 mm. The samples were vacuum-dried at 60 °C overnight and kept at a relative humidity (RH) of 0% (conditioned by P_2O_5) for 7 days. After weighing, they were conditioned at room temperature in a desiccator of 98% RH (conditioned by $CuSO_4{\cdot}5H_2O$ saturated solution). Seven days later, the samples were removed and weighed. The moisture uptake (Mu) of the samples was calculated as the weight-increas-

ing percent after being conditioned for 7 days at 98% of RH (Cao et al. 2007).

3. Results and discussion

3.1. Morphology of the NPS granules and PSN

SEM photograph of NPS granules and the TEM photograph of PSN are shown in Fig. 1. The native pea starch granules are in a shape of approximate ellipse with a size of about 25–30 μm (Fig. 1a). After the acid-treatment process, the granules have been destructed and degraded to be nanocrystals with a size range of 30–80 nm (Fig. 1b). For the first time, the pea starch nanocrystals, prepared from native pea starch granules according to the previous optimization process (Angellier et al., 2004), showed very close morphological characteristics to the starch nanocrystals from waxy maize starch (Angellier et al., 2004; Putaux et al., 2003).

3.2. FTIR analysis

The FTIR spectra of the original materials and selected films are shown in Fig. 2. The main absorption peaks in the spectrum of NPS, PSN, PVA/NPS-*n*, PVA/PSN-*n* ($n = 10$ and 30) and PVA are listed in Table 1. The main characteristic peaks of starch in NPS are consistent with that of the previous reports (Jayasekara et al., 2004; Yin et al., 2005; Zhang & Han, 2006). The stretching and bending vibration of the hydrogen bonding —OH group of starch occurred at 3276 and 1650 cm^{-1}, respectively. The stretching vibration of C—O bond in C—O—H and C—O—C group in the anhydrous glucose ring appeared at 1150, 1077, and 990 cm^{-1}. The characteristic peak of C—O—C ring vibration in starch located at 760 cm^{-1}. After the acid hydrolysis, the above-mentioned peaks at 3276, 1650, 1150, 1077, 990, and 760 cm^{-1} in NPS shifted to 3368, 1644, 1155, 1078, 1016, and 768 cm^{-1} in PSN, respectively. The other details of changes in FTIR spectra after hydrolysis are listed in Table 1. Most of the changes in spectrum are related to the hydrogen bonding in starch molecules, indicating the hydrolysis treatment significantly changed the inter- and intra-molecular hydrogen bonding of starch molecules.

In the FTIR spectrum of PVA shown in Fig. 2, the stretching and bending vibration of —OH absorption peaks occurred at around 3292 and 1654 cm^{-1}, respectively. The characteristic peaks at 1733 and 1713 cm^{-1} in PVA are attributed to the residual acetate groups due to the manufacture of PVA from hydrolysis of polyvinyl acetate (Jayasekara et al., 2004). The location and assignment of the other main peaks shown in Fig. 2 are in accord with the reported literature (Hemantha Kumar et al., 2004; Naidu, Sairam, Raju, & Aminabhavi, 2005).

It was observed from Fig. 2 and Table 1 that the peak at around 760 cm^{-1} was the characteristic absorption of starch, and the peak at 1733 cm^{-1} was the characteristic absorption of PVA, which were not overlapped by other absorption peaks. The two peaks existed together in the FTIR spectra of the PVA/NPS-*n* and PVA/PSN-*n* films, indicating the success of blending of PVA with NPS and PSN, respectively. However by comparison with the original spectra of NPS, PSN, and PVA, the corresponding absorption peaks in the spectra of the blend films have shifted as shown in Table 1. These changes are due to the plasticization of glycerol and the interactions between PVA and starch molecules in the blending and film-form-

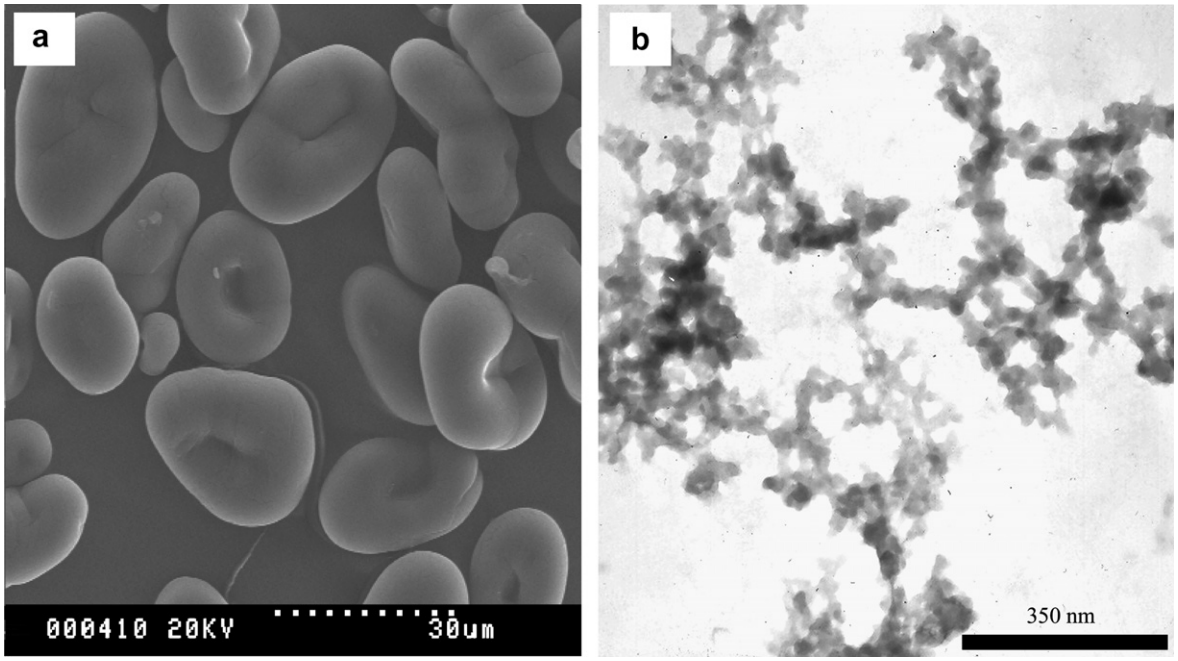

Fig. 1. SEM photograph (a) of NPS granules and TEM photograph (b, scale bar: 350 nm) of PSN.

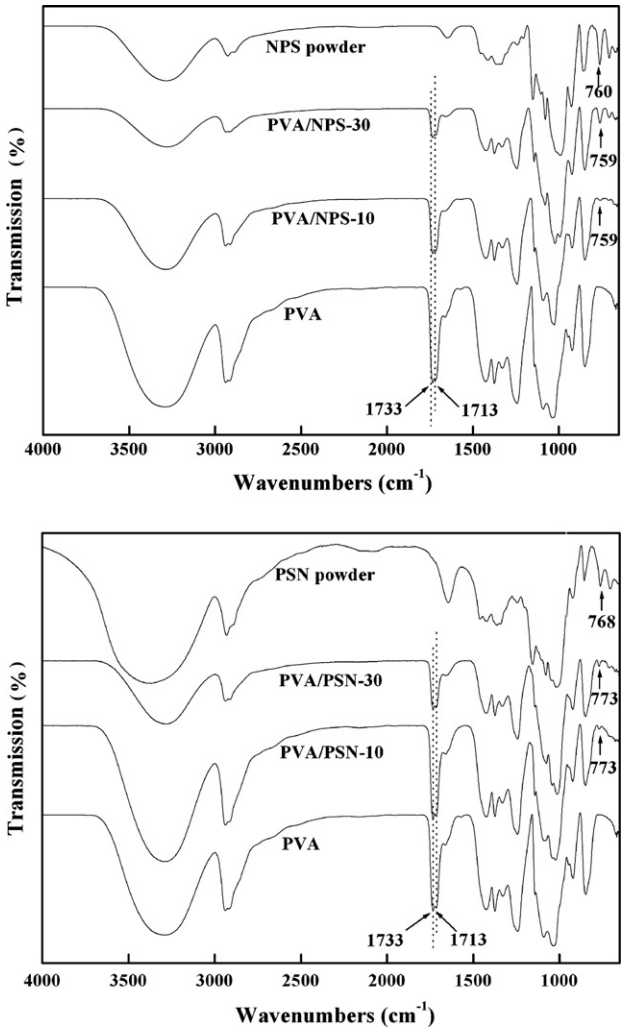

Fig. 2. FTIR spectra of NPS and PSN powders, PVA, PVA/NPS-*n*, and PVA/PSN-*n* ($n = 10$ and 30) films.

ing process. However, it is worth noting that the shape and location of the main peaks in PVA/NPS-*n* and PVA/PSN-*n* were closer to these in PVA. This suggests the interactions of PVA–PVA molecules dominated and were stronger than that of PVA–starch molecules and starch–starch molecules in the blending system.

3.3. XRD analysis

The XRD patterns of the original materials and resulting films are shown in Fig. 3, and the corresponding data are listed in Table 2. NPS granules, from field pea, have the characteristic typical C-type crystalline pattern containing A-type and B-type polymorphs like other legume starches (Hoover & Ratnayake, 2002; Ratnayake et al., 2002). As shown in Fig. 3, NPS exhibited a middle intensity diffraction peak at 5.4° (characteristic of B-type polymorphs), two strong intensity peaks at 17.8° and 19.4°, and two weak intensity peaks at 14.8° and 21.2°. Following the acid hydrolysis treatment, obvious changes happened in the diffraction pattern of PSN. The typical B-type polymorph peaks at 5.4° and 19.4° of NPS almost disappeared, while new peaks at 9.7°, 11.4°, 17.8°, 22.9°, and 23.8° appeared. It is worth noting that all the new peaks in the PSN were assigned to the A-type polymorph of starch (Cairns, Bogracheva, Ring, Hedley, & Morris, 1997). These indicate that PSN hydrolyzed from NPS was mainly A-type polymorph. It has been reported that field pea starches contain pure A- and B-type polymorphs in varying proportions (Hoover & Ratnayake, 2002). During the acid hydrolysis process, acid attacked amorphous areas more rapidly than the crystalline ones (Putaux et al., 2003). For the crystalline areas, B-type polymorph disappeared ahead of A-type polymorph, indicating much less B-type polymorph content than A-type one in the starch granules. Furthermore, the peak at 21.2° shifted to 22.9° in PSN, and became very sharp, which is associated with an increase in crystalline regions and with losses in amorphous fractions (Puchongkavarin, Bergthaller, Shobsngob, & Varavinit, 2003). The result of XRD shows that A-type polymorph of the starch crystalline still remained during the acid hydrolysis process, accompanied by the loss of amorphous and B-type polymorph in original NPS granules.

PVA showed an obvious diffraction peak at 19.4° (García-Cerda, Escareño-Castro, & Salazar-Zertuche, 2007; Ma, Qian, Yin, & Zhu, 2002). In the blend of PVA/NPS-*n*, most of the peaks in NPS were not observed and the diffraction patterns were very close to that of PVA. This is

Table 1
Peak assignment in the FTIR spectra of NPS and PSN powders, PVA, PVA/NPS-*n*, and PVA/PSN-*n* ($n = 10$ and 30) films

Peak assignment	NPS powder	PSN powder	PVA/NPS-10	PVA/NPS-30	PVA/PSN-10	PVA/PSN-30	PVA
—OH (st)	3276	3368	3287	3281	3292	3280	3292
C=O (st) (characteristic carbonyl vibration in the residue acetate in PVA)	–	–	1733	1733	1733	1733	1733
	–	–	1713	1713	1713	1713	1713
—OH (b)	1650	1644	1656	1643	1656	1652	1654
C—O (st) in C—O—H	1150	1155	1143	1143	1143	1143	–
	1077	1078	1090	1078	1087	1074	1091
C—O (st) in C—O—C	990	1016	1026	1026	1022	1013	1035
C—O (b) (characteristic C—O—C ring vibration in starch)	760	768	760	760	765	773	–

St, stretching; b, bending.

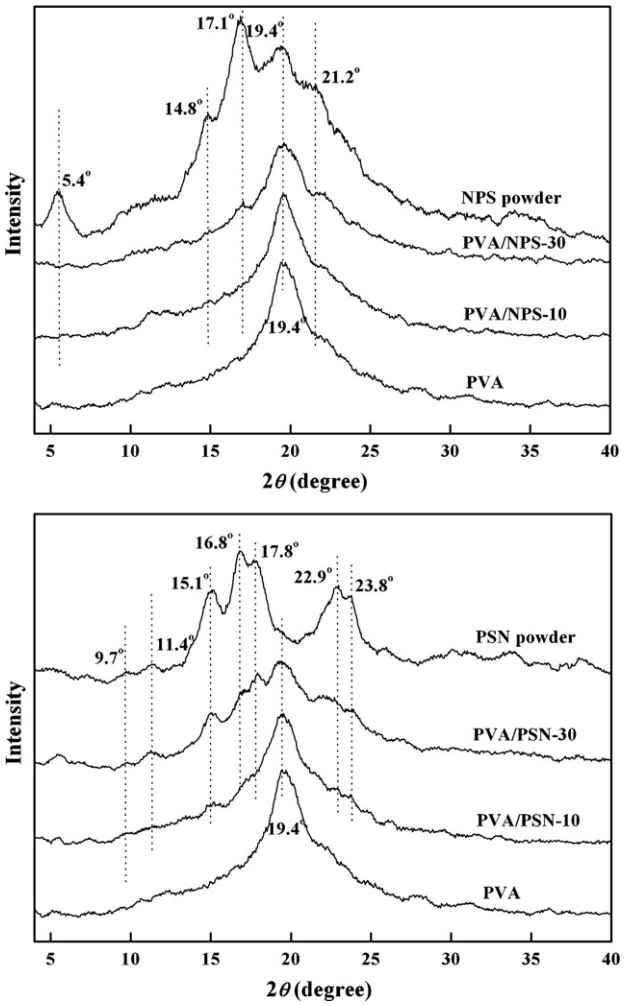

Fig. 3. XRD patterns of NPS and PSN powders, PVA, PVA/NPS-*n*, and PVA/PSN-*n* ($n = 10$ and 30) films.

due to the destruction of crystalline structure of starch granules as a result of gelatinization during the blending process with PVA at 100 °C. No obvious retrogradation of starch was observed from the XRD patterns, indicating that the diffraction pattern of PVA dominated in the blends and that the crystalline structure of starch has been strongly inhibited by PVA and glycerol molecules.

The main peaks at 19.5° in PVA/PSN-10 and 19.3° in PVA/PSN-30 were from PVA because no corresponding peak was found in PSN. On the whole, the XRD patterns of PVA/PSN-*n* were also very close to that of PVA. But the peaks at 15.1°, 17.8°, and 22.9° in PSN still existed in the PVA/PSN-*n* blend films. This was different from the XRD diffraction pattern of PVA/NPS-*n*. It indicate that the crystalline structure of PSN still remained in the blend films because the crystallinity of starch nanocrystals was preserved during the blending process at room temperature and evaporating process at 40 °C (Angellier et al., 2006). All the other diffraction peaks such as that at 9.7°, 11.4°, 17.8°, and 23.8° of PSN should appear in the PVA/PSN-*n* films if there was no strong interaction between PVA and PSN molecules in the blend films (Jia et al., 2007). However, the peaks at 9.7°, 11.4°, 17.8°, and 23.8° in PSN were not observed in the PVA/PSN-10 and PVA/PSN-30; and the peaks at 15.0°, 17.9°, and 22.0° from PSN in the blend films were very weak. It is attributed to the interactions of PVA and PSN in the composites. In other words, the crystalline of starch nanocrystals remained during the hydrolyzing process but disappeared or weakened in the film-forming process, showing that the diffraction pattern of PVA dominated in the composite and the crystalline of starch nanocrystals has been partly prohibited by the strong interactions between PVA and PSN molecules.

3.4. Morphology of the films

The SEM photographs of the cross-sections of PVA, PVA/NPS-*n*, and PVA/PSN-*n* ($n = 10$, 20, 30, and 40) films are shown in Fig. 4. It was observed that the cross-sections of pure PVA film were smooth, while the PVA/NPS-*n* composite films became rougher with an increase of NPS content. Obvious aggregations of starch and micro-phase separation between PVA and starch appeared in the cross-section of PVA/NPS-40 film. The cross-sections of the PVA/PSN-*n* nanocomposites were also relatively rougher than PVA film. However, they were much smoother than the corresponding PVA/NPS-*n* films. Especially, in the nanocomposites with PSN content less than

Table 2
The data of the XRD diffraction patterns of NPS and PSN powders, PVA, PVA/NPS-*n*, and PVA/PSN-*n* ($n = 10$ and 30) films

Type of the polymorphs		NPS powder	PSN powder	PVA/NPS-10	PVA/NPS-30	PVA/PSN-10	PVA/ PSN-30	PVA
Peaks from starch	B-type	5.4	–	–	–	–	–	–
	A-type	–	9.7	–	–	–	–	–
	A-type	–	11.4	–	–	–	11.3	–
	A- and B-type	14.8	15.1	–	–	15.2	15.0	–
	A- and B-type	16.9	16.8	–	17.0	–	–	–
	A-type	–	17.8	–	–	–	17.9	–
	B-type	19.4	–	–	–	–	–	–
	B-type	21.2	–	–	–	–	–	–
	A-type	–	22.9	–	–	–	22.0	
	A-type	–	23.8	–	–	–		–
Peaks from starch and PVA	–	–	–	19.6	19.6	–	–	–
Peaks from PVA	–	–	–	–	–	19.5	19.3	19.4

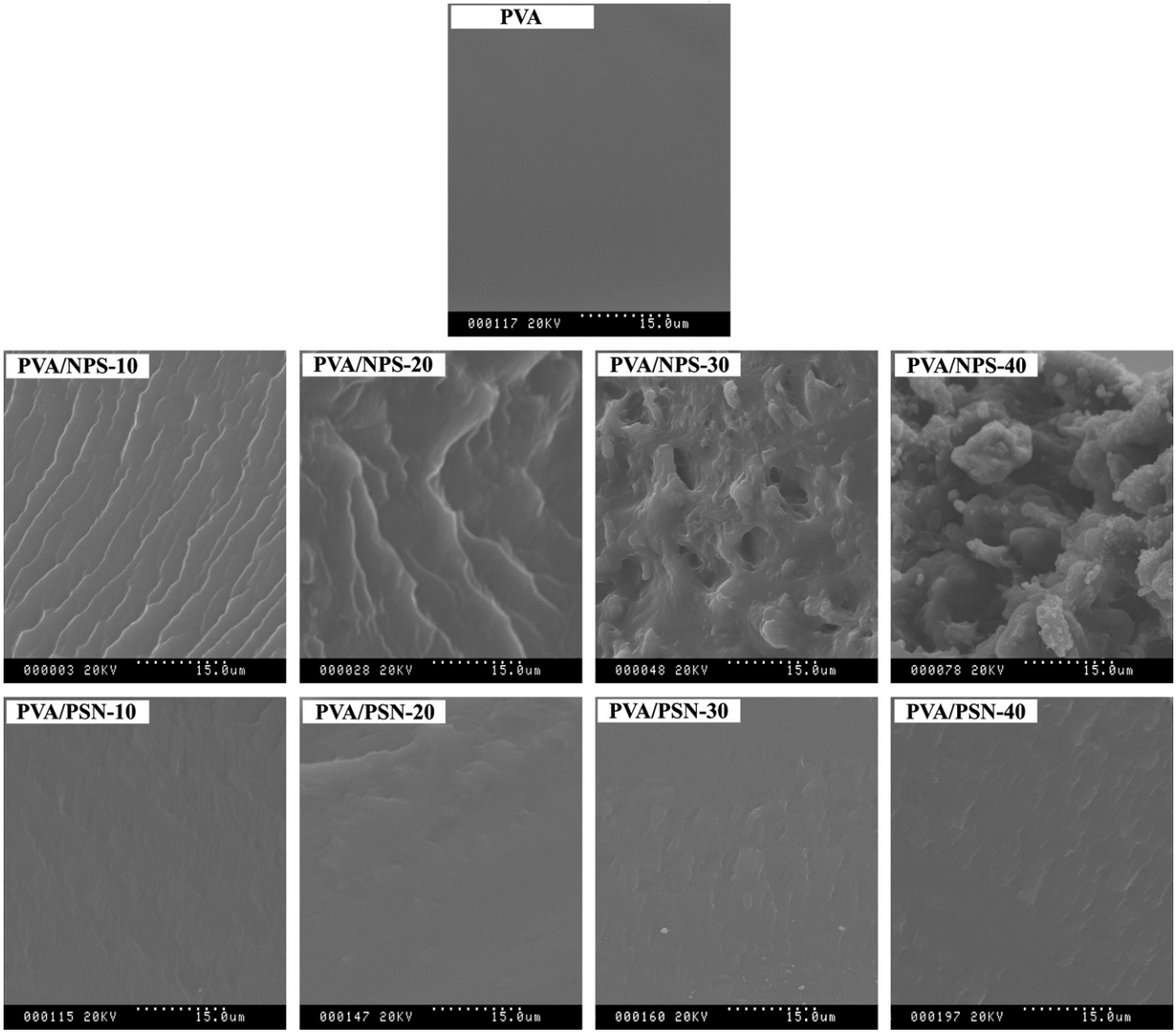

Fig. 4. SEM photographs of the cross-sections of PVA, PVA/NPS-*n*, and PVA/PSN-*n* ($n = 10$, 20, 30, and 40) films.

30 wt%, no obvious aggregations of nanocrystals and microphase separation were observed from SEM photographs. This indicates that PSN dispersed more homogenously than NPS in PVA matrix, resulting in a more chances to interact with PVA, and thus formed a stronger interaction and adhesion on the interfaces of PSN and PVA molecules.

3.5. Light transmittance testing

The light transmittance (Tr) of the selective films at the wavelength from 200 to 800 nm is shown in Fig. 5. The films obviously showed higher Tr values at the range of visible light (400–800 nm) than that at the range of ultraviolet light (200–400 nm). The Tr values of PVA, PVA/PSN-5, and PVA/PSN-25 films are higher than 83% at the wavelength from 400 to 800 nm, indicating their good transparency in nature. At the same wavelength, the Tr of PVA/PSN-5 is the highest among the selected films, due to the homogeneous dispersion of PSN and strong interactions with PVA. With an increase of NPS from 5 to 25 wt%, the Tr values of the composite films decreased significantly. However, with an increase of PSN from 5 to 25 wt%, the Tr values of the composite films decreased slightly. This is due to the different size of NPS and PSN, which exhibited different interactions with PVA and resulted in different effects on the optical properties of the composite films.

In our experiments, the obtained PVA and PVA/PSN-*n* films were transparent in appearance, while the PVA/NPS-*n* films with NPS content higher than 10 wt% were opaque. The Tr value at 800 nm can reflect the transparency of the films and the transparency provides information on the particle size of dispersed particle in matrix (Kampeerapappun et al., 2007; Wang, Du, Luo, Lin, & Kennedy, 2007). The dependence of Tr of the films at 800 nm on the content of NPS or PSN is shown in Fig. 6. The Tr of the PVA film

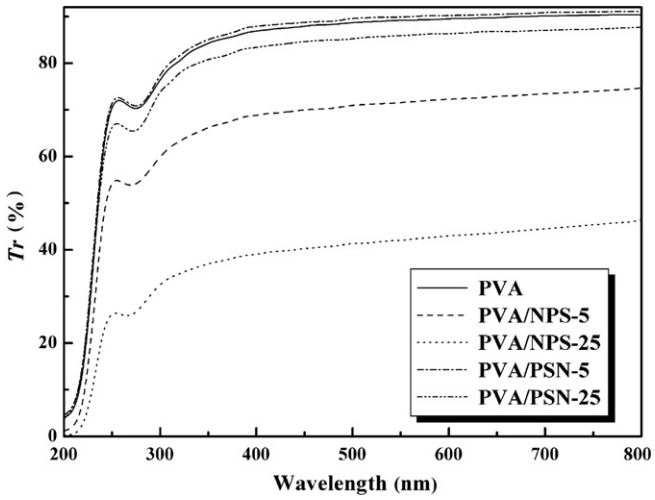

Fig. 5. Dependence of the light transmittance (Tr) of PVA, PVA/NPS-*n*, and PVA/PSN-*n* ($n = 5$ and 25) films on the wavelength from 200 to 800 nm.

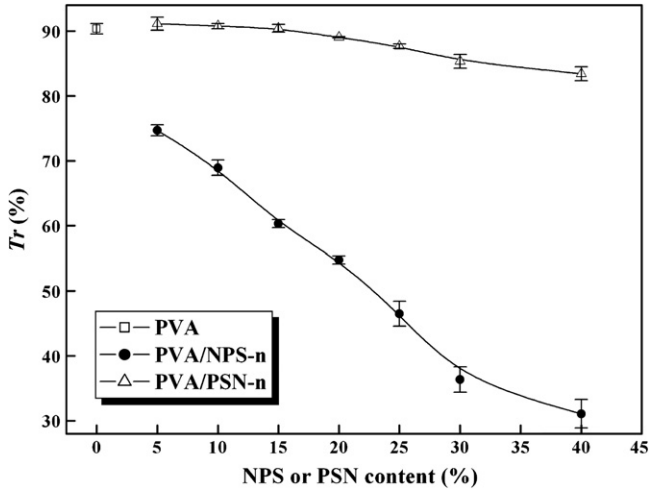

Fig. 6. Light transmittance (Tr) of PVA, PVA/NPS-*n*, and PVA/PSN-*n* films at wavelength of 800 nm.

was 90.4%, and the Tr of the blend films ranged from 91.1% to 83.4% for PVA/PSN-*n* films, and from 74.7% to 31.1% for PVA/NPS-*n* films, respectively. With an increase of PSN or NPS content in the films, the Tr decreased. Particularly, the decrease tendency of Tr in PVA/NPS-*n* films was more rapid. The much lower Tr value of PVA/NPS-*n* films was a hint of bigger particle size of NPS, poorer compatibility and increased phase separation between PVA and NPS (Siddaramaiah et al., 2004; Yin et al., 2005). In contrast, the Tr of the PVA/PSN-*n* films with PSN content less than 30 wt% was very close to and even slightly higher than that of pure PVA film. Furthermore, the Tr of the PVA/PSN-*n* film was much higher than that of the corresponding PVA/NPS-*n* films. This strongly proves that PSN with a nanometer size dispersed homogeneously in PVA matrix and formed strong interactions with PVA molecules in the blending and film-forming process, resulting in good compatibility and retention of transparency of PVA in the blending films.

3.6. Mechanical properties of the films

Fig. 7 shows the tensile strength (σ_b) and elongation at break (ε_b) of PVA and composite films. The values of σ_b and ε_b of the PVA film were 37 MPa and 710%, respectively. As reported by most of the researchers, the values of σ_b and ε_b of the PVA/NPS films were lower than that of PVA film, and decreased with an increase of starch content (Ramaraj, 2007b). It indicates that the addition of starch granule could not improve the mechanical properties of the composites because of the excellent mechanical properties of PVA itself and the poor compatibility of PVA and starch in nature.

The tensile strength and elongation at break of the PVA/PSN-5 and PVA/PSN-10 films were slightly higher than that of pure PVA film, indicating that the mechanical properties of the composite films were slightly improved when the content of PSN incorporated was lower than

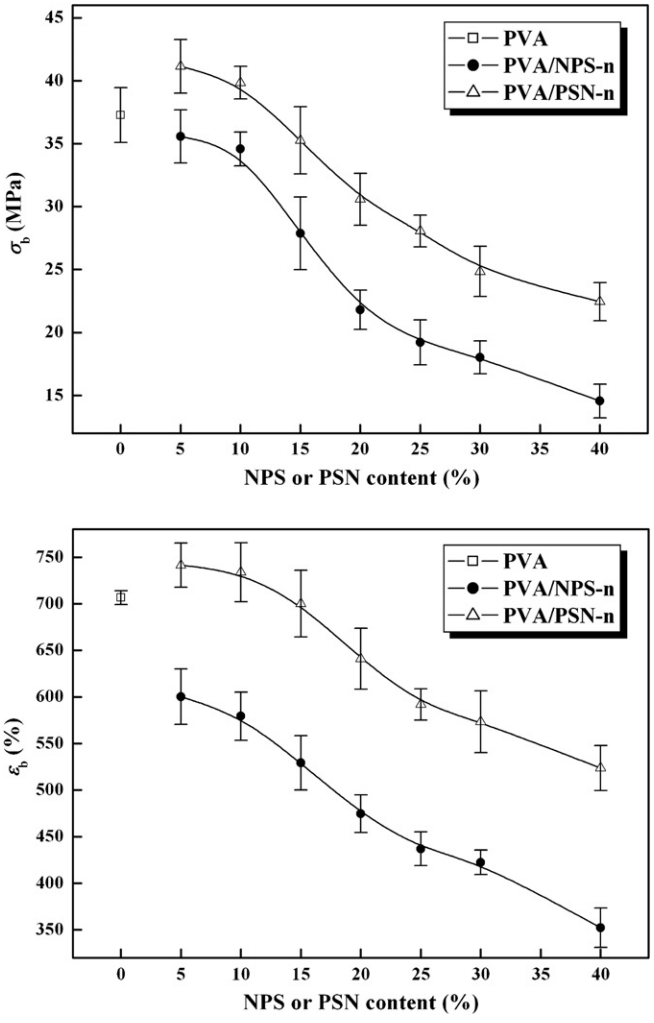

Fig. 7. Tensile strength (σ_b) and elongation at break (ε_b) of PVA, PVA/NPS-*n*, and PVA/PSN-*n* films.

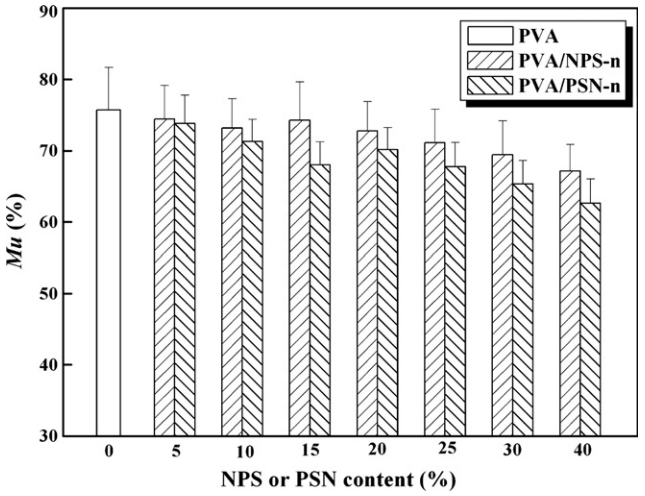

Fig. 8. Moisture uptake (Mu) of PVA, PVA/NPS-*n*, and PVA/PSN-*n* films at RH of 98% for 7 days.

10 wt%. With an increase of PSN, the values of σ_b and ε_b of the PVA/PSN-*n* films decreased and became lower than that of PVA film. However, the σ_b and ε_b of the PVA/PSN-*n* nanocomposite films were higher than that of the corresponding PVA/NPS-*n* composite films. This further proves that starch nanocrystals with smaller size dispersed more homogeneously and formed stronger interactions with PVA molecules than native starch granules did during the film-forming process. The results from tensile testing are very consistent with that from SEM observation and light transmittance testing.

3.7. Moisture uptake testing

PVA is water-soluble and starch is water-sensitive, which results in the water-sensitivity of their blends. Thus any decrease of water-sensitivity for the blend films is very meaningful for the applications of the films. The moisture uptake (Mu) of the films at 7 days under 98% RH is shown in Fig. 8. All the Mu of the blend films was lower than that of the PVA. On the whole, with an increase of NPS or PSN content, the Mu of the blend films decreased. For example, the Mu of PVA film was about 78% while that of the PVA/NPS-40 and PVA/PSN-40 film was about 67% and 62%, respectively. Furthermore, the Mu of PVA/PSN-*n* films was lower than that of the corresponding PVA/NPS-*n* films. This is attributed to the higher crystallinity of PSN than that of NPS, and the stronger interactions between PSN and PVA than that between NPS and PVA in the composite films.

4. Conclusions

Pea starch nanocrystals (PSN) dispersion was prepared from native pea starch (NPS) by hydrolyzing with sulfuric acid. The size of PSN was in the range of 30–80 nm. Two series of composite films were prepared from NPS and PSN, respectively, with PVA by a casting and evaporation process. Compared with pure PVA film, the PVA/NPS films exhibited a certain degree of decreased light transmittance and mechanical properties, improved water-resistivity and lowered cost. The PVA/PSN nanocomposite films containing 5 and 10 wt% of PSN content possessed improved physical properties than pure PVA film. More interestingly, the PVA/PSN nanocomposite films showed smoother fracture surfaces, higher light transmittance, higher tensile strength and elongation at break, and lower moisture uptake than the corresponding PVA/NPS composite films. This is due to that PSN, compared with NPS, has smaller size and dispersed more homogeneously in PVA matrix, resulting in stronger interactions with PVA. This work explored new applications of native pea starch and its nanocrystals as low-cost fillers. It also provided starch-modified PVA composites with different structure and properties.

Acknowledgement

This work was financially supported by Canadian Biomass Innovation Network (CBIN) TID 824 project.

References

Angellier, H., Choisnard, L., Molina-Boisseau, S., Ozil, P., & Dufresne, A. (2004). Optimization of the preparation of aqueous suspensions of waxy maize starch nanocrystals using a response surface methodology. *Biomacromolecules, 5*(4), 1545–1551.

Angellier, H., Molina-Boisseau, S., & Dufresne, A. (2005). Mechanical properties of waxy maize starch nanocrystal reinforced natural rubber. *Macromolecules, 38*(22), 9161–9170.

Angellier, H., Molina-Boisseau, S., Dole, P., & Dufresne, A. (2006). Thermoplastic starch–waxy maize starch nanocrystals nanocomposites. *Biomacromolecules, 7*(2), 531–539.

Beliakova, M. K., Aly, A. A., & Abdel-Mohdy, F. A. (2004). Grafting of poly(methacrylic acid) on starch and poly(vinyl alcohol). *Starch/Stäke, 56*(9), 407–412.

Cairns, P., Bogracheva, T. Y., Ring, S. G., Hedley, C. L., & Morris, V. J. (1997). Determination of the polymorphic composition of smooth pea starch. *Carbohydrate Polymers, 32*(3–4), 215–282.

Cao, X., Chen, Y., Chang, P. R., & Huneault, M. A. (2007). Preparation and properties of plasticized starch/multiwalled carbon nanotubes composites. *Journal of Applied Polymer Science, 106*(2), 1431–1437.

Çaykara, T., & Demirci, S. (2006). Preparation and characterization of blend films of poly(vinyl alcohol) and sodium alginate. *Journal of Macromolecular Science, Part A: Pure and Applied Chemistry, 43*(7), 1113–1121.

Cinelli, P., Chiellini, E., Lawton, J. W., & Imam, S. H. (2006). Foamed articles based on potato starch, corn fibers and poly(vinyl alcohol). *Polymer Degradation and Stability, 91*(5), 1147–1155.

Corti, A., Cinelli, P., D'Antone, S., Kenawy, E., & Solaro, R. (2002). Biodegradation of poly(vinyl alcohol) in soil environment: Influence of natural organic fillers and structural parameters. *Macromolecular Chemistry and Physics, 203*(10–11), 1526–1531.

Dubief, D., Samain, E., & Dufresne, A. (1999). Polysaccharide microcrystals reinforced amorphous poly(b-hydroxyoctanoate) nanocomposite materials. *Macromolecules, 32*(18), 5765–5771.

Dufresne, A., & Cavaillé, J. (1998). Clustering and percolation effects in microcrystalline starch-reinforced thermoplastic. *Journal of Polymer Science, Part B: Polymer Physics, 36*(12), 2211–2224.

Dufresne, A., Cavaillé, J., & Helbert, W. (1996). New nanocomposite materials: Microcrystalline starch reinforced thermoplastic. *Macromolecules, 29*(23), 7624–7626.

Fernandes, D. M., Hechenleitner, A. A. W., Job, A. E., Radovanocic, E., & Pineda, E. A. G. (2006). Thermal and photochemical stability of poly(vinyl alcohol)/modified lignin blends. *Polymer Degradation and Stability, 91*(5), 1192–1201.

Follain, N., Joly, C., Dole, P., & Bliard, C. (2005a). Properties of starch based blends. Part 2. Influence of poly vinyl alcohol addition and photocrosslinking on starch based materials mechanical properties. *Carbohydrate Polymers, 60*(2), 185–192.

Follain, N., Joly, C., Dole, P., & Bliard, C. (2005b). Mechanical properties of starch-based materials. I. Short review and complementary experimental analysis. *Journal of Applied Polymer Science, 97*(5), 1783–1794.

García-Cerda, L. A., Escareño-Castro, M. U., & Salazar-Zertuche, M. (2007). Preparation and characterization of polyvinyl alcohol–cobalt ferrite nanocomposites. *Journal of Non-Crystalline Solids, 353*(8–10), 808–810.

Hemantha Kumar, G. N., Lakshmana Rao, J., Gopal, N. O., Narasimhulu, K. V., Chakradhar, R. P. S., & Varada Rajulu, A. (2004). Spectroscopic investigations of Mn^{2+} ions doped polyvinylalcohol films. *Polymer, 45*(16), 5407–5415.

Hoover, R., & Ratnayake, W. S. (2002). Starch characteristics of black bean, chick pea, lentil, navy bean and pinto bean cultivars grown in Canada. *Food Chemistry, 78*(4), 489–498.

Imam, S. H., Cinelli, P., Gordon, S. H., & Chiellini, E. (2005). Characterization of biodegradable composite films prepared from blends of poly(vinyl alcohol), cornstarch, and lignocellulosic fiber. *Journal of Polymers and the Environment, 13*(1), 47–55.

Jayasekara, R., Harding, I., Bowater, I., Christie, G. B. Y., & Lonergan, G. T. (2004). Preparation, surface modification and characterisation of solution cast starch PVA blended films. *Polymer Testing, 23*(1), 17–27.

Jia, Y. T., Gong, J., Gu, X. H., Kim, H. Y., Dong, J., & Shen, X. Y. (2007). Fabrication and characterization of poly (vinyl alcohol)/chitosan blend nanofibers produced by electrospinning method. *Carbohydrate Polymers, 67*(3), 403–409.

Kampeerapappun, P., Aht-ong, D., Pentrakoon, D., & Srikulkit, K. (2007). Preparation of cassava starch/montmorillonite composite film. *Carbohydrate Polymers, 67*(2), 155–163.

Khan, M. A., Bhattacharia, S. K., Kader, M. A., & Bahari, K. (2006). Preparation and characterization of ultra violet (UV) radiation cured bio-degradable films of sago starch/PVA blend. *Carbohydrate Polymers, 63*(4), 500–506.

Lawton, J. W. (1996). Effect of starch type on the properties of starch containing films. *Carbohydrate Polymers, 29*(3), 203–208.

Lenz, R. W. (1993). Biodegradable polymers. *Advances in Polymer Science, 107*, 1–40.

Lu, Y., Weng, L., & Zhang, L. (2004). Morphology and properties of soy protein isolate thermoplastics reinforced with chitin whiskers. *Biomacromolecules, 5*(3), 1046–1051.

Ma, X., Qian, X., Yin, J., & Zhu, Z. (2002). Preparation and characterization of polyvinyl alcohol-selenide nanocomposites at room temperature. *Journal of Materials Chemistry, 12*(3), 663–666.

Mohanty, A. K., Misra, M., & Hinrichsen, G. (2000). Biofibres, biodegradable polymers and biocomposites: An overview. *Macromolecular Materials and Engineering, 276–277*(1), 1–24.

Nabar, Y. U., Draybuck, D., & Narayan, R. (2006). Physicomechanical and hydrophobic properties of starch foams extruded with different biodegradable polymers. *Journal of Applied Polymer Science, 102*(1), 58–68.

Naidu, B. V. K., Sairam, M., Raju, K. V. S. N., & Aminabhavi, T. M. (2005). Pervaporation separation of water + isopropanol mixtures using novel nanocomposite membranes of poly(vinyl alcohol) and polyaniline. *Journal of Membrane Science, 260*(1–2), 142–155.

Paillet, M., & Dufresne, A. (2001). Chitin whisker reinforced thermoplastic nanocomposites. *Macromolecules, 34*(19), 6527–6530.

Paradossi, G., Cavalieri, F., Chiessi, E., Spagnoli, C., & Cowman, M. K. (2003). Poly(vinyl alcohol) as versatile biomaterial for potential biomedical applications. *Journal of Materials Science: Materials in Medicine, 14*(8), 687–691.

Pšeja, J., Charvátová, H., Hruzík, P., Hrnčiřík, J., & Kupec, J. (2006). Anaerobic biodegradation of blends based on polyvinyl alcohol. *Journal of Polymers and the Environment, 14*(2), 185–190.

Puchongkavarin, H., Bergthaller, W., Shobsngob, S., & Varavinit, S. (2003). Characterization and utilization of acid-modified rice starches for use in pharmaceutical tablet compression. *Starch/Stärke, 55*(10), 464–475.

Putaux, J., Molina-Boisseau, S., Momaur, T., & Dufresne, A. (2003). Platelet nanocrystals resulting from the disruption of waxy maize starch granules by acid hydrolysis. *Biomacromolecules, 4*(5), 1198–1202.

Ramaraj, B. (2006). Modified poly(vinyl alcohol) and coconut shell powder composite films: Physico-mechanical, thermal properties, and swelling studies. *Polymer – Plastics Technology and Engineering, 45*(11), 1227–1231.

Ramaraj, B. (2007a). Crosslinked poly(vinyl alcohol) and starch composite films.II. physicomechanical, thermal properties and swelling studies. *Journal of Applied Polymer Science, 103*(2), 909–916.

Ramaraj, B. (2007b). Crosslinked poly(vinyl alcohol) and starch composite films: Study of their physicomechanical, thermal, and swelling properties. *Journal of Applied Polymer Science, 103*(2), 1127–1132.

Ratnayake, W. S., Hoover, R., & Warkentin, T. (2002). Pea starch: Composition, structure and properties – A review. *Starch/Stärch, 54*(6), 217–234.

Samir, M. A. S. A., Alloin, F., Gorecki, W., Sanchez, J., & Dufresne, A. (2004). Nanocomposite polymer electrolytes based on poly(oxyethylene) and cellulose nanocrystals. *Journal of Physical Chemistry B, 108*(30), 10845–10852.

Siddaramaiah, S., Raj, B., & Somashekar, R. (2004). Structure–property relation in polyvinyl alcohol/starch composites. *Journal of Applied Polymer Science, 91*(1), 630–635.

Sreedhar, B., Chattopadhyay, D. K., Karunakar, M. S. H., & Sastry, A. R. K. (2006). Thermal and surface characterization of plasticized starch polyvinyl alcohol blends crosslinked with epichlorohydrin. *Journal of Applied Polymer Science, 101*(1), 25–34.

Su, J. F., Huang, Z., Liu, K., Fu, L. L., & Liu, H. R. (2007). Mechanical properties, biodegradation and water vapor permeability of blend films of soy protein isolate and poly (vinyl alcohol) compatibilized by glycerol. *Polymer Bulletin, 58*(5–6), 913–921.

Wang, X., Du, Y., Luo, J., Lin, B., & Kennedy, J. F. (2007). Chitosan/organic rectorite nanocomposite films: Structure, characteristic and drug delivery behaviour. *Carbohydrate Polymers, 69*(1), 41–49.

Yi, F., Lu, J. W., Guo, Z. X., & Yu, J. (2004). Mechanical properties and biocompatibility of soluble eggshell membrane protein/poly(vinyl alcohol) blend films. *Journal of Biomaterials Science, Polymer Edition, 17*(9), 1015–1024.

Yin, Y., Li, J., Liu, Y., & Li, Z. (2005). Starch crosslinked with poly(vinyl alcohol) by boric acid. *Journal of Applied Polymer Science, 96*(4), 1394–1397.

Zhai, M., Yoshii, F., & Kume, T. (2003). Radiation modification of starch-based plastic sheets. *Carbohydrate Polymers, 52*(3), 311–317.

Zhang, Y., & Han, J. H. (2006). Plasticization of pea starch gilms with monosaccharides and polyols. *Journal of Food Science, 71*(6), E253–E261.

Zhang, X., Burgar, I., Lourbakos, E., & Beh, H. (2004). The mechanical property and phase structures of wheat proteins/polyvinyl alcohol blends studied by high-resolution solid-state NMR. *Polymer, 45*(10), 3305–3312.